

# Detecting Preformed-Pair Current through Nonequilibrium Noise in the BCS–BEC Crossover

Hiroyuki Tajima,<sup>1,\*</sup> Daigo Oue,<sup>2,3</sup> Mamoru Matsuo,<sup>3,4,5,6</sup> and Takeo Kato<sup>7</sup>

<sup>1</sup>*Department of Physics, Graduate School of Science,  
The University of Tokyo, Tokyo, 113-0033, Japan*

<sup>2</sup>*The Blackett Laboratory, Department of Physics, Imperial College London,  
Prince Consort Road, Kensington, London SW7 2AZ, United Kingdom*

<sup>3</sup>*Kavli Institute for Theoretical Sciences, University of Chinese Academy of Sciences, Beijing, 100190, China.*

<sup>4</sup>*CAS Center for Excellence in Topological Quantum Computation,  
University of Chinese Academy of Sciences, Beijing 100190, China*

<sup>5</sup>*Advanced Science Research Center, Japan Atomic Energy Agency, Tokai, 319-1195, Japan*

<sup>6</sup>*RIKEN Center for Emergent Matter Science (CEMS), Wako, Saitama 351-0198, Japan*

<sup>7</sup>*Institute for Solid State Physics, University of Tokyo, Kashiwa 277-8581, Japan*

(Dated: February 9, 2022)

We theoretically propose a method to identify the tunneling current carrier in interacting fermions from nonequilibrium noise in the Bardeen-Cooper-Schrieffer to Bose–Einstein condensate crossover. The noise-to-current ratio, the Fano factor, can be a crucial probe for the current carrier. Bringing strongly-correlated fermions into contact with a dilute reservoir produces a tunneling current in between. The associated Fano factor increases from one to two as the interaction becomes stronger, reflecting the formation of the preformed Cooper pairs or bound molecules.

*Introduction*— Transport phenomena have contributed to the development of the fundamental physics in previous centuries. Various unconventional phenomena such as superfluidity and superconductivity were observed using transport measurements. However, clarifying the microscopic mechanism of the transport phenomena in strongly-correlated systems remains challenging because of their complexities such as strong interactions, lattice geometries, as well as multiple degrees of freedom.

Recently, an ultracold atomic system has been regarded as a quantum simulator for strongly-correlated many-body systems such as unconventional superconductors and nuclear systems, owing to its controllability of physical parameters (e.g., interparticle interactions and lattice structures) and its cleanliness, called *atomtronics* [1]. In particular, state-of-the-art experiments for tunneling current have been conducted in strongly interacting Fermi gases [2–7]. These experiments motivate us to study tunneling transport associated with the Josephson effect and Cooper-pair tunneling in the superfluid phase of the Bardeen-Cooper-Schrieffer (BCS) to Bose–Einstein-condensate (BEC) crossover [8–15].

One crucial problem is to determine how strong correlations affect transport quantities in the normal phase near the critical temperature (e.g., preformed pair and pseudogap [16]). Recently, several theoretical efforts have been paid to understand anomalous tunneling current induced by pairing fluctuations in the normal phase [17–20], as observed in experiments [2–7]. It is reported that such anomalous pair currents can be induced by the nonlinear one-body tunneling processes [17], the one-body tunneling of a closed-channel molecule in the two-channel model [18], and the proximity effect associated with two-body interactions [21]. In this sense, it is worth exploring

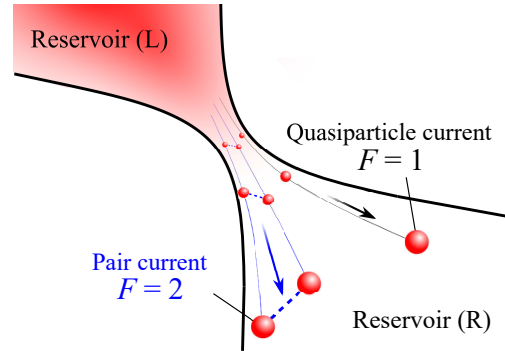


FIG. 1. Strongly interacting quantum gases (reservoirs L and R) with a large chemical-potential bias in between. The Fano factor  $F$  can be regarded as an indicator of the current carrier, i.e., quasiparticle current ( $F = 1$ ) and the pair current ( $F = 2$ ).

clear evidence for anomalous pair currents in a strongly interacting Fermi gas above the superfluid critical temperature.

For this purpose, measuring the Fano factor is promising, which is defined by a current and the associated nonequilibrium noise [22, 23]. The Fano factor in the large-biased setup reflects the effective charge per elementary transport process. The most fascinating example is the detection of fractional charges in fractional quantum Hall systems [24, 25]. The Fano factor has been used to determine the effective charge (or spin) in various physical systems such as superconductors [26, 27], Kondo quantum dots [28, 29], and magnetic junctions [30–33].

In this study, we show that the Fano factor  $F$  can be used as a probe for the current carrier in the BCS–BEC crossover. Figure 1 shows a schematic setup of the large-

biased system. Using the many-body  $T$ -matrix approach (TMA) [34, 35], we numerically calculate the current and nonequilibrium noise within the Schwinger–Keldysh approach in the two-terminal tunneling junction under a large bias. Furthermore, we reveal how the Fano factor  $F$  changes in a strongly-interacting regime, thereby reflecting the change of the dominant carrier. Our result can be tested by cold-atom experiments for which the noise measurement has been theoretically proposed [36]. Moreover, the Fano factor provides a direct evidence of pair-fluctuation effects associated with preformed pairs rather than other measurements such as spin susceptibility and photoemission spectra previously studied in this field [16]. The current-noise measurement can also be used to identify the carriers of the BCS–BEC crossover in condensed-matter systems such as FeSe semimetal [37–40], lithium-intercalated layered nitrides [41, 42], magic-angle twisted trilayer graphene [43], and organic superconductor [44]. Moreover, the noise measurement has recently been conducted in a copper oxide heterostructure [45, 46] and disordered superconductor [47].

In the following, we take  $\hbar = k_B = 1$  and consider a unit volume.

*Formalism*— We consider the Hamiltonian  $H = H_L + H_R + H_{1T} + H_{2T}$ . The reservoir Hamiltonian  $H_{j=L,R}$  is given by

$$H_j = \sum_{\mathbf{p},\sigma} \xi_{\mathbf{p},j} c_{\mathbf{p},\sigma,j}^\dagger c_{\mathbf{p},\sigma,j} + g \sum_{\mathbf{q}} P_{\mathbf{q},j}^\dagger P_{\mathbf{q},j}, \quad (1)$$

where  $\xi_{\mathbf{p},j} = p^2/(2m) - \mu_j$  denotes the kinetic energy measured from the chemical potential  $\mu_j$  and  $c_{\mathbf{p},\sigma,j}$  denotes the annihilation operator of a Fermi atom with momentum  $\mathbf{p}$  and the pseudospin  $\sigma = \uparrow, \downarrow$ . The second term in Eq. (1) denotes the attractive interaction with a contact-type coupling  $g$ , where  $P_{\mathbf{q},j} = \sum_{\mathbf{p}} c_{-\mathbf{p}+\mathbf{q}/2,\downarrow,j} c_{\mathbf{p}+\mathbf{q}/2,\uparrow,j}$  is the pair-annihilation operator and  $g$  is related to the scattering length  $a$  as  $\frac{m}{4\pi a} = \frac{1}{g} + \sum_{\mathbf{p}} \frac{m}{p^2}$  [35].

The one-body tunneling Hamiltonian,

$$H_{1T} = \sum_{\mathbf{p},\mathbf{k},\sigma} \left[ t_{\mathbf{p},\mathbf{k}} c_{\mathbf{p},\sigma,L}^\dagger c_{\mathbf{k},\sigma,R} + \text{h.c.} \right], \quad (2)$$

is associated with the one-body potential barrier, where  $t_{\mathbf{p},\mathbf{k}}$  denotes its coupling strength. The two-body tunneling Hamiltonian reads

$$H_{2T} = \sum_{\mathbf{q},\mathbf{q}'} \left[ w_{\mathbf{q},\mathbf{q}'} P_{\mathbf{q},L}^\dagger P_{\mathbf{q}',R} + \text{h.c.} \right], \quad (3)$$

where  $w_{\mathbf{q},\mathbf{q}'}$  is the two-body coupling strength, induced by the local interaction term in Eq. (1) combined with the one-body potential barrier [21]. Such two-body tunneling processes can be obtained within the one-body tunneling of a closed-channel molecule in the two-channel model [18] and the multiple one-body tunneling processes in the non-linear regime [14, 17, 20, 48]. Similar tunneling effects have also been examined in one-dimensional

few-body systems [49, 50]. Here, we do not go into details on the origin of the one- and two-body tunneling, but rather investigate their possible consequence in observable quantities.

Using the Schwinger–Keldysh approach, we evaluate the expectation values of the current operator  $\hat{I} = i[\hat{N}_L, H]$  ( $\hat{N}_j = \sum_{\mathbf{p},\sigma} c_{\mathbf{p},\sigma,j}^\dagger c_{\mathbf{p},\sigma,j}$  denotes the density operator in the  $j$ -reservoir) in the steady state at the lowest-order tunneling couplings by a sum of the one- and two-body contributions as  $I = I_{\text{qp}} + I_{\text{pair}}$ , where each component reads [21, 51]

$$\begin{aligned} I_{\text{qp}} &= \int_{-\infty}^{\infty} \frac{d\omega}{2\pi} \sum_{\mathbf{p},\mathbf{k},\sigma} |t_{\mathbf{k},\mathbf{p}}|^2 \mathcal{A}_{\mathbf{k},L}(\omega) \mathcal{A}_{\mathbf{p},R}(\omega) \\ &\quad \times [f_L(\omega) - f_R(\omega)], \\ I_{\text{pair}} &= 2 \int_{-\infty}^{\infty} \frac{d\omega}{2\pi} \sum_{\mathbf{q},\mathbf{q}'} |w_{\mathbf{q},\mathbf{q}'}|^2 \mathcal{B}_{\mathbf{q},L}(\omega) \mathcal{B}_{\mathbf{q}',R}(\omega) \\ &\quad \times [b_L(\omega) - b_R(\omega)]. \end{aligned} \quad (4)$$

In Eq. (4),  $\mathcal{A}_{\mathbf{k},j}(\omega)$  and  $\mathcal{B}_{\mathbf{q},j}(\omega)$  denote one- and two-particle spectral functions, respectively,  $f_j(\omega)$  and  $b_j(\omega)$  denotes the Fermi and Bose distribution functions, and  $\mu_{\text{b},j} = 2\mu_j$  denotes the bosonic-pair chemical potential in the  $j$ -reservoir. We define the current noise  $\mathcal{S}$  as

$$\mathcal{S} = \frac{1}{2} \int_{-\infty}^{\infty} dt \left( \langle \hat{I}(t) \hat{I}(0) \rangle + \langle \hat{I}(0) \hat{I}(t) \rangle \right). \quad (5)$$

Similar to the calculation above, we can evaluate the current noise [51] as the sum of the two contributions:  $\mathcal{S} = \mathcal{S}_{\text{qp}} + \mathcal{S}_{\text{pair}}$ , where

$$\begin{aligned} \mathcal{S}_{\text{qp}} &= \int_{-\infty}^{\infty} \frac{d\omega}{2\pi} \sum_{\mathbf{p},\mathbf{k},\sigma} |t_{\mathbf{k},\mathbf{p}}|^2 \mathcal{A}_{\mathbf{k},L}(\omega) \mathcal{A}_{\mathbf{p},R}(\omega) \\ &\quad \times [f_L(\omega) \{1 - f_R(\omega)\} + \{1 - f_L(\omega)\} f_R(\omega)], \\ \mathcal{S}_{\text{pair}} &= 4 \int_{-\infty}^{\infty} \frac{d\omega}{2\pi} \sum_{\mathbf{q},\mathbf{q}'} |w_{\mathbf{q},\mathbf{q}'}|^2 \mathcal{B}_{\mathbf{q},L}(\omega) \mathcal{B}_{\mathbf{q}',R}(\omega) \\ &\quad \times [b_L(\omega) \{1 + b_R(\omega)\} + b_R(\omega) \{1 + b_L(\omega)\}], \end{aligned} \quad (6)$$

In the large bias limit ( $\Delta\mu \equiv \mu_L - \mu_R \rightarrow \infty$ ), we can prove  $\mathcal{S}_{\text{qp}}/I_{\text{qp}} = 1$  and  $\mathcal{S}_{\text{pair}}/I_{\text{pair}} = 2$  without any further approximations [51]. This motivates us to consider the Fano factor,

$$F = \frac{\mathcal{S}}{I} = \frac{\mathcal{S}_{\text{qp}} + \mathcal{S}_{\text{pair}}}{I_{\text{qp}} + I_{\text{pair}}}. \quad (7)$$

The Fano factor  $F$  changes from 1 to 2, according to whether the quasiparticle or pair tunneling is dominant and hence, it is a useful probe for the current carrier. In particular, the Fano factor  $F$  becomes 1 and 2 in the BCS limit ( $a^{-1} \rightarrow -\infty$ ) and BEC limit ( $a^{-1} \rightarrow \infty$ ), respectively.

To demonstrate this, we employ the many-body TMA to calculate spectral functions  $\mathcal{A}_{\mathbf{k},j}(\omega)$ ,  $\mathcal{B}_{\mathbf{q},j}(\omega)$ , and  $\mu_j$  for

given densities  $N_j$  in the BCS–BEC crossover regime [35]. The single-particle propagator is given by

$$G_{\mathbf{k},j}(i\omega_n) = \frac{1}{G_{\mathbf{k},j}^0(i\omega_n)^{-1} - \Sigma_{\mathbf{k},j}(i\omega_n)}, \quad (8)$$

$$\Sigma_{\mathbf{k},j}(i\omega_n) = T_j \sum_{\mathbf{q},\ell} \Gamma_{\mathbf{q},j}(i\nu_\ell) G_{\mathbf{q}-\mathbf{k},j}^0(i\nu_\ell - i\omega_n), \quad (9)$$

where  $G_{\mathbf{k},j}^0(i\omega_n) = (i\omega_n - \xi_{\mathbf{k},j})^{-1}$  denotes the bare propagator and  $\Sigma_{\mathbf{k},j}(i\omega_n)$  denotes the TMA self-energy. Following a standard TMA procedure [52], the  $T$ -matrix  $\Gamma_{\mathbf{q},j}(i\nu_\ell)$  is formulated by incorporating the particle–particle multiple scattering as

$$\Gamma_{\mathbf{q},j}(i\nu_\ell) = g [1 - g\Pi_{\mathbf{q},j}(i\nu_\ell)]^{-1}, \quad (10)$$

using the bare two-body propagator given as

$$\Pi_{\mathbf{q},j}(i\nu_\ell) = -T_j \sum_{\mathbf{p},n} G_{\mathbf{p}+\mathbf{q}/2,j}^0(i\omega_n + i\nu_\ell) G_{-\mathbf{p}+\mathbf{q}/2,j}^0(-i\omega_n). \quad (11)$$

The fermion (boson) Matsubara frequency is denoted by  $\omega_n$  ( $\nu_\ell$ ). Furthermore, we define the dressed two-body propagator [53] as

$$\mathcal{G}_{\mathbf{q},j}(i\nu_\ell) = \Pi_{\mathbf{q},j}(i\nu_\ell) [1 + \Pi_{\mathbf{q},j}(i\nu_\ell)\Gamma_{\mathbf{q},j}(i\nu_\ell)]. \quad (12)$$

The spectral functions can be obtained from the analytic continuation as  $\mathcal{A}_{\mathbf{k},j}(\omega) = -2 \text{Im} G_{\mathbf{k},j}(i\omega_n \rightarrow \omega - \mu_j + i\eta)$  and  $\mathcal{B}_{\mathbf{q},j}(\omega) = -2 \text{Im} \mathcal{G}_{\mathbf{q},j}(i\nu_\ell \rightarrow \omega - \mu_{b,j} + i\eta)$  with an infinitesimal small number  $\eta$ .

In this study, we consider the large bias regime (see Fig. 1) characterized by  $\mu_L - \mu_R \rightarrow \infty$  [51, 54] and the momentum-conserved tunneling processes as  $t_{\mathbf{p},\mathbf{k}} = \mathcal{T}_1 \delta_{\mathbf{p},\mathbf{k}}$  and  $w_{\mathbf{q},\mathbf{q}'} = \mathcal{T}_2 \delta_{\mathbf{q},\mathbf{q}'}$ , for simplicity. We employ  $\eta = 10^{-2} E_{F,L}$  in the numerical calculation to avoid the divergent behavior of the current associated with the momentum-conserved tunneling in the weak- and strong-coupling limits, where  $E_{F,L} = (3\pi^2 N_L)^{2/3} / (2m)$  denotes the Fermi energy of the L reservoir with the number density  $N_L$ . However, our result can be qualitatively unchanged by this treatment because the distribution functions play a key role in determining  $F$  rather than the detailed structures of tunneling junctions. Moreover,  $\mathcal{T}_2$  must be normalized to suppress the ultraviolet divergence in  $B_{\mathbf{q},j}(\omega)$ . For this purpose, we introduce the renormalized two-body tunneling coupling  $\mathcal{T}_{2,\text{ren.}} = \frac{\Lambda^2 k_{F,L}}{3\pi^2} \mathcal{T}_2$  where  $k_{F,L} = \sqrt{2mE_{F,L}}$  denotes the Fermi momentum. Such a divergence can also be avoided by introducing the form factor for the relative momentum  $\mathbf{p}$  in  $P_{\mathbf{q},j}$  [55]. In this work, we take  $\Lambda = 100k_{F,L}$  [35] in the practical calculation.

*Results*— Fig. 2 shows the Fano factor  $F$  as a function of the dimensionless interaction parameter  $(k_{F,L}a)^{-1}$  in the entire BCS-BEC crossover regime above the superfluid critical temperature  $T_c$ . We considered  $\mathcal{T}_{2,\text{ren.}}/\mathcal{T}_1 =$

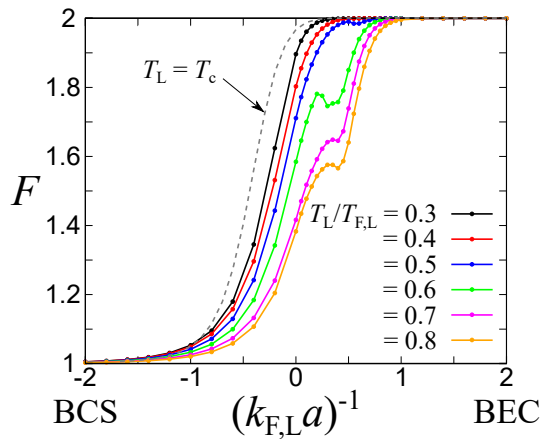


FIG. 2. Fano factor  $F$ , associated with tunneling transport between two reservoirs, throughout the BCS-BEC crossover for various temperatures  $T_L$ . The reservoir R is almost vacuum. The ratio between tunneling couplings is given as  $\mathcal{T}_{2,\text{ren.}}/\mathcal{T}_1 = 1$ . For comparison, we plot the result at  $T_L = T_c$  (dashed curve). Note that  $T_c$  changes in the range of  $0.02T_{F,L} \lesssim T_c \lesssim 0.24T_{F,L}$  depending on  $(k_{F,L}a)^{-1}$ .

1, and the reservoir R was regarded as almost vacuum ( $\mu_L - \mu_R \rightarrow \infty$ ) [51]. One can clearly see that  $F$  evolves from 1 to 2 with increasing the interaction strength in Fig. 2, indicating that the current carrier gradually changes from quasiparticles ( $F = 1$ ) to preformed Cooper pair or bound molecules ( $F = 2$ ). Such a behavior is universal in the sense that these asymptotic values do not depend on any details on the model parameters and structures of tunneling junctions. More explicitly, at the large bias limit, one can obtain [51]

$$F(\Delta\mu \rightarrow \infty) \rightarrow \frac{I_{\text{qp}} + 2I_{\text{pair}}}{I_{\text{qp}} + I_{\text{pair}}}, \quad (13)$$

where  $I_{\text{qp}}$  and  $I_{\text{pair}}$  denote the contributions of the quasiparticle and pair tunnelings, respectively. The Fano factor  $F$  approaches 1 and 2 in the quasiparticle-dominant ( $I_{\text{qp}} \gg I_{\text{pair}}$ ) and pair-dominant regimes ( $I_{\text{pair}} \gg I_{\text{qp}}$ ), respectively. Although the interaction dependence of the Fano factor  $F$  is deeply related to properties of the tunneling junctions and spectral functions of the carriers, one can find from Eq. (13) that  $F \rightarrow 1$  ( $F \rightarrow 2$ ) in the limit of  $a^{-1} \rightarrow -\infty$  ( $a^{-1} \rightarrow \infty$ ) regardless of the detailed properties of the system. Moreover,  $F = 2$  can be realized even above  $T_c$  because of strong interactions leading to the formation of preformed Cooper pairs in the BCS–BEC crossover. With increasing the temperature,  $F$  tends to be suppressed because thermal effects assist the dissociation of pairs. Nevertheless, even at finite temperature,  $F$  approaches 2 with increasing the interaction because bound molecules are dominant in the deep BEC regime where  $T_L \lesssim E_b$  [ $E_b = 1/(ma^2)$  is the two-body binding energy].

To see the detailed behavior of the Fano factor  $F$ , we

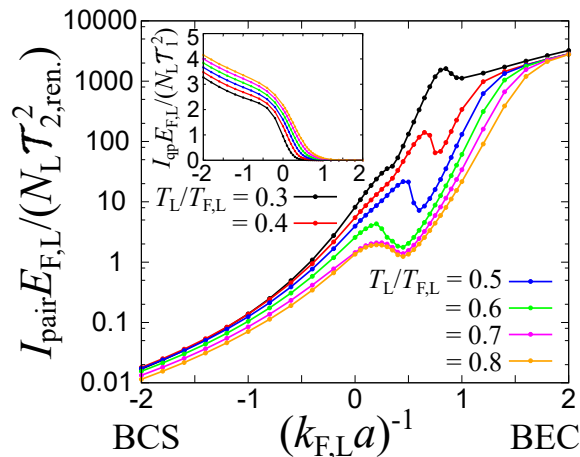


FIG. 3. Preformed-pair current  $I_{\text{pair}}$  in the normal phase throughout the BCS-BEC crossover at different temperatures. The inset shows the quasiparticle current  $I_{\text{qp}}$  with the same horizontal axis  $(k_{\text{F,L}}a)^{-1}$ .

plot  $I_{\text{qp}}$  and  $I_{\text{pair}}$  throughout the BCS-BEC crossover at different temperatures in Fig. 3. From the inset of Fig. 3, the quasiparticle current  $I_{\text{qp}}$  is exponentially suppressed with increasing the attractive interaction  $(k_{\text{F,L}}a)^{-1} > 0$ . This suppression is induced by the pseudogap effect, i.e., the reduction of  $\mathcal{A}_{\mathbf{k},\text{L}}(\omega)$  near  $|\mathbf{k}| = k_{\text{F,L}}$  and  $\omega = E_{\text{F,L}} (\simeq \mu_{\text{L}})$  by the particle-hole coupling. Finally,  $I_{\text{qp}}$  approaches zero in the BEC limit  $((k_{\text{F,L}}a)^{-1} \rightarrow \infty)$  because of the formation of molecules with large binding energies. These results are qualitatively consistent with previous work [17, 20]. On the other hand,  $I_{\text{pair}}$  drastically increases with increasing the interaction strength  $(k_{\text{F,L}}a)^{-1}$  as shown in Fig. 3. At the BCS side  $((k_{\text{F,L}}a)^{-1} < 0)$  where the attraction is not strong to form a two-body bound state in vacuum, the contribution of  $I_{\text{pair}}$  can be regarded as the tunneling of the preformed Cooper pairs into the two-body continuum in the reservoir R. In the strong-coupling BEC regime  $((k_{\text{F,L}}a)^{-1} > 1$  and  $T_{\text{L}}/E_{\text{b}} \lesssim 1)$ ,  $I_{\text{pair}}$  describes the tunneling transport of bound molecules across two reservoirs, because the two-body bound state exists in the reservoir R with the same coupling  $g$ . Such a tunneling current associated with weakly-interacting molecular bosons becomes large due to their long lifetime and the Bose enhancement of low-energy distributions.

One can also see a dip-hump structure of  $I_{\text{pair}}$  in the intermediate regime. Here,  $\mu_{\text{L}}$  is close to zero and changes its sign, indicating that the dominant contribution changes from the preformed-pair transfer to the molecule-to-molecule transport across the junction. From the unitary limit  $((k_{\text{F,L}}a)^{-1} = 0)$ , the preformed-pair transfer increases due to the overlap with the bound-state spectra in  $\mathcal{B}_{\mathbf{q},\text{R}}(\omega)$  and eventually decreases because of the decrease in  $\mu_{\text{L}}$ . With increasing the interaction further, the inter-reservoir molecule-to-molecule

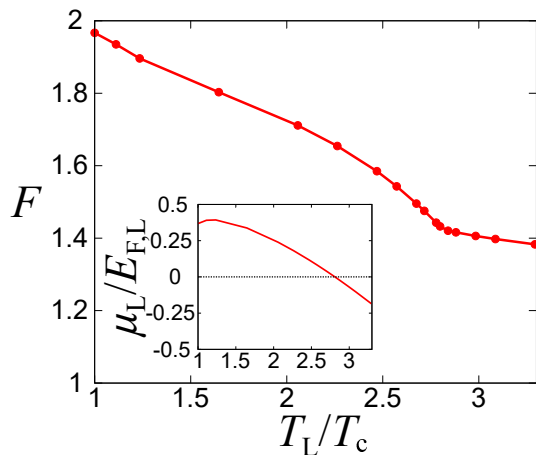


FIG. 4. Temperature dependence of the Fano factor  $F$  in the unitary limit  $[1/(k_{\text{F,L}}a) = 0]$  with  $\mathcal{T}_{2,\text{ren.}}/\mathcal{T}_1 = 1$ . The horizontal axis is taken as  $T_{\text{L}}/T_{\text{c}}$ , where  $T_{\text{c}}$  is the superfluid critical temperature. The inset shows the chemical potential  $\mu_{\text{L}}$  as a function of  $T_{\text{L}}/T_{\text{c}}$  for a given Fermi energy  $E_{\text{F,L}}$ .

transition emerges where the bound-state spectra in two reservoirs get close to each other in the energy axis  $\omega$ . Although these structures reflect the physical properties of the system, they also depend on the detailed setup of the tunneling junctions (e.g., the ratio between the tunneling couplings  $\mathcal{T}_{2,\text{ren.}}/\mathcal{T}_1$ ) [51].

Figure 4 shows the temperature dependence of the Fano factor  $F$  in the unitary limit  $((k_{\text{F,L}}a)^{-1} = 0)$ . Because  $\mathcal{B}_{\mathbf{q},\text{R}}(\omega)$  does not involve a bound molecule pole, the transfer of the preformed Cooper pairs in the reservoir L to the scattering two-body continuum in the reservoir R can be anticipated in the unitary limit. One can see the enhancement of the Fano factor  $F$  at the low-temperature regime. In particular, the curvature of the Fano factor  $F$  is modified at  $T_{\text{L}}/T_{\text{c}} \simeq 2.8$ , where the sign of  $\mu_{\text{L}}$  changes from negative to positive one as the temperature decreases (see the inset of Fig. 4). At a positive  $\mu_{\text{L}}$ , the pole of the preformed Cooper pairs gradually appears in  $\mathcal{B}_{\mathbf{q},\text{L}}(\omega)$ . Thus, the behavior of the Fano factor  $F$  can be regarded as a signature of the emergence of the preformed Cooper pairs. Because the preformed Cooper pairs play an important role in the pseudogap physics of ultracold Fermi gases [16], the Fano factor contributes to the further understanding of pairing pseudogaps in the BCS-BEC crossover regime. Incidentally, because TMA does not capture the self-energy shift in  $\Pi_{\mathbf{q},\text{L}}(\omega)$ , the curvature change of the Fano factor  $F$  may differ from the temperature where  $\mu_{\text{L}} = 0$  in actual experiments and in more sophisticated theoretical approaches [34, 35].

*Summary*— In this study, we showed that the Fano factor (i.e., the noise-to-current ratio  $F = \mathcal{S}/I$ ) can be a useful probe for current carriers in the BCS-BEC crossover at large-biased tunneling junctions. Using the many-body TMA, we demonstrated that the Fano factor

$F$  gradually changes from one to two as the interaction strength increases in the normal phase, indicating that the dominant current carrier changes from the quasiparticle ( $F = 1$ ) to the pair ( $F = 2$ ) along the BCS-BEC crossover. Our prediction can be tested by experiments and uncover nonequilibrium strong-coupling physics via transport measurements. Furthermore, our result indicates that the noise measurement is useful for the study

of the BCS-BEC crossover and pair-fluctuation effects in unconventional superconductors.

This work is supported in part by Grants-in-Aid for Scientific Research from JSPS (Grants Nos. JP18H05406, JP20K03831). D.O. is funded by the President's PhD Scholarships at Imperial College London. MM is partially supported by the Priority Program of the Chinese Academy of Sciences, Grant No. XDB28000000.

### Schwinger-Keldysh approach for current and noise

We start from the current operator given by

$$\hat{I} = \hat{I}_{\text{qp}} + \hat{I}_{\text{pair}}, \quad (14)$$

$$\hat{I}_{\text{qp}} = i \sum_{\mathbf{p}, \mathbf{k}, \sigma} t_{\mathbf{k}, \mathbf{p}} \left[ c_{\mathbf{k}, \sigma, \text{L}}^\dagger c_{\mathbf{p}, \sigma, \text{R}} - c_{\mathbf{p}, \sigma, \text{R}}^\dagger c_{\mathbf{k}, \sigma, \text{L}} \right], \quad (15)$$

$$\hat{I}_{\text{pair}} = 2i \sum_{\mathbf{q}, \mathbf{q}'} w_{\mathbf{q}, \mathbf{q}'} \left[ P_{\mathbf{q}, \text{L}}^\dagger P_{\mathbf{q}', \text{R}} - P_{\mathbf{q}', \text{R}}^\dagger P_{\mathbf{q}, \text{L}} \right], \quad (16)$$

where  $\hat{I}_{\text{qp}}$  and  $\hat{I}_{\text{pair}}$  are operators for quasiparticle and pair currents, respectively. Truncating the higher-order contributions with respect to the tunneling Hamiltonians [i.e.,  $O(H_{1\text{T}}^3)$ ,  $O(H_{2\text{T}}^3)$ ], we can evaluate their expectation values,  $I_{\text{qp}}(t_1, t_2) = \langle \Psi(t_1) | \hat{I}_{\text{qp}} | \Psi(t_2) \rangle$  and  $I_{\text{pair}}(t_1, t_2) = \langle \Psi(t_1) | \hat{I}_{\text{pair}} | \Psi(t_2) \rangle$ , for the different times  $t_1$  and  $t_2$ , where  $|\Psi(t)\rangle$  is the state-vector of the steady state. First, the quasiparticle contribution reads

$$I_{\text{qp}}(t_1, t_2) = -2 \int_C dt' \sum_{\mathbf{p}, \mathbf{k}, \sigma} |t_{\mathbf{k}, \mathbf{p}}|^2 \text{Re} \left[ \langle T_C c_{\mathbf{k}, \sigma, \text{R}}(t_2) c_{\mathbf{k}, \sigma, \text{R}}^\dagger(t') \rangle \langle T_C c_{\mathbf{p}, \sigma, \text{L}}(t') c_{\mathbf{p}, \sigma, \text{L}}^\dagger(t_1) \rangle \right], \quad (17)$$

where  $C$  denotes the Keldysh contour. Note that while the right hand side of Eq. (17) depends only on  $t_1 - t_2$  in considering the steady state. Using the Green's functions, we rewrite  $I_{\text{qp}}(t_1, t_2)$  as

$$I_{\text{qp}}(t_1, t_2) = 2 \int_{-\infty}^{\infty} dt' \sum_{\mathbf{p}, \mathbf{k}, \sigma} |t_{\mathbf{k}, \mathbf{p}}|^2 \text{Re} \left[ G_{\mathbf{p}, \text{R}}^{\text{ret.}}(t_2 - t') G_{\mathbf{k}, \text{L}}^<(t' - t_1) + G_{\mathbf{p}, \text{R}}^<(t_2 - t') G_{\mathbf{k}, \text{L}}^{\text{adv.}}(t' - t_1) \right], \quad (18)$$

where  $G^{\text{ret. (adv.)}}$  is the retarded (advanced) Green's function of a fermion in thermal equilibrium. The lesser component  $G^<$  contains the information of the thermal distribution in each reservoir. Here, we take  $t_1 = t_2 \equiv t$  and the Fourier transformation

$$I_{\text{qp}} = 2 \int \frac{d\omega}{2\pi} \sum_{\mathbf{p}, \mathbf{k}, \sigma} |t_{\mathbf{k}, \mathbf{p}}|^2 \text{Re} \left[ G_{\mathbf{p}, \text{R}}^{\text{ret.}}(\omega) G_{\mathbf{k}, \text{L}}^<(\omega) + G_{\mathbf{p}, \text{R}}^<(\omega) G_{\mathbf{k}, \text{L}}^{\text{ret.*}}(\omega) \right]. \quad (19)$$

Moreover, we use

$$G_{\mathbf{k}, \text{j}}^<(\omega) = -2i f_{\text{j}}(\omega) \text{Im} G_{\mathbf{k}, \text{j}}^{\text{ret.}}(\omega) \equiv i f_{\text{j}}(\omega) \mathcal{A}_{\mathbf{k}, \text{j}}(\omega), \quad (20)$$

where

$$f_{\text{j}}(\omega) = \frac{1}{\exp(\frac{\omega - \mu_{\text{j}}}{T_{\text{j}}}) + 1} \quad (21)$$

is the Fermi-Dirac distribution function. We use Matsubara Green's functions in each reservoir reaching thermal equilibrium as a grand-canonical ensemble with  $-\mu_{\text{j}} \hat{N}_{\text{j}}$  and obtain the retarded(advanced) Green's function by the analytic continuation with  $\mu_{\text{j}}$  as  $i\omega_n \rightarrow \omega + i\eta - \mu_{\text{j}}$  in each reservoir. Then, we obtain

$$I_{\text{qp}} = \int \frac{d\omega}{2\pi} \sum_{\mathbf{p}, \mathbf{k}, \sigma} |t_{\mathbf{k}, \mathbf{p}}|^2 \mathcal{A}_{\mathbf{p}, \text{L}}(\omega) \mathcal{A}_{\mathbf{k}, \text{R}}(\omega) [f_{\text{L}}(\omega) - f_{\text{R}}(\omega)]. \quad (22)$$

Similarly, we obtain the pair current contribution as

$$I_{\text{pair}} = 2 \sum_{\mathbf{q}, \mathbf{q}'} \int \frac{d\omega}{2\pi} |\omega_{\mathbf{q}, \mathbf{q}'}|^2 \mathcal{B}_{\mathbf{q}, \text{L}}(\omega) \mathcal{B}_{\mathbf{q}', \text{R}}(\omega) [b_{\text{L}}(\omega) - b_{\text{R}}(\omega)], \quad (23)$$

where we used the relation for the two-particle Green's function given  $\mathcal{G}^<$  by

$$\mathcal{G}_{\mathbf{q}, \text{j}}^<(\omega) = 2ib_{\text{j}}(\omega) \text{Im} \mathcal{G}_{\mathbf{q}, \text{j}}^{\text{ret.}}(\omega) \equiv -ib_{\text{j}}(\omega) \mathcal{B}_{\mathbf{q}, \text{j}}(\omega), \quad (24)$$

and the Bose-Einstein distribution function

$$b_{\text{j}}(\omega) = \frac{1}{\exp\left(\frac{\omega - \mu_{\text{b}, \text{j}}}{T_{\text{j}}}\right) - 1}, \quad (25)$$

with a bosonic (pair) chemical potential  $\mu_{\text{b}, \text{j}} = 2\mu_{\text{j}}$ .  $\mathcal{G}^{<(>)}$  and  $\mathcal{G}^{\text{ret.}(\text{adv.})}$  are the lesser (greater) and retarded (advanced) components of two-particle Green's functions, respectively. One can find that  $I = I_{\text{qp}} + I_{\text{pair}}$  obtained from Eqs. (17) and (23) is equivalent to Eq. (4).

Next, we consider the current noise

$$\mathcal{S} = \frac{1}{2} \int_{-\infty}^{\infty} dt \left( \langle \hat{I}(t) \hat{I}(0) \rangle + \langle \hat{I}(0) \hat{I}(t) \rangle \right). \quad (26)$$

At lowest order of tunneling couplings, we obtain

$$\begin{aligned} \langle \hat{I}(t) \hat{I}(0) \rangle &= \sum_{\mathbf{p}, \mathbf{k}, \sigma} |t_{\mathbf{p}, \mathbf{k}}|^2 \left[ G_{\mathbf{k}, \text{L}}^<(t) G_{\mathbf{p}, \text{R}}^>(-t) + G_{\mathbf{p}, \text{R}}^<(t) G_{\mathbf{k}, \text{L}}^>(-t) \right] \\ &\quad - 4 \sum_{\mathbf{q}, \mathbf{q}'} |w_{\mathbf{q}, \mathbf{q}'}|^2 \left[ \mathcal{G}_{\mathbf{q}, \text{L}}^<(t) \mathcal{G}_{\mathbf{q}', \text{R}}^>(-t) + \mathcal{G}_{\mathbf{q}', \text{R}}^<(t) \mathcal{G}_{\mathbf{q}, \text{L}}^>(-t) \right], \end{aligned} \quad (27)$$

$$\begin{aligned} \langle \hat{I}(0) \hat{I}(t) \rangle &= \sum_{\mathbf{p}, \mathbf{k}, \sigma} |t_{\mathbf{p}, \mathbf{k}}|^2 \left[ G_{\mathbf{k}, \text{L}}^<(-t) G_{\mathbf{p}, \text{R}}^>(t) + G_{\mathbf{p}, \text{R}}^<(-t) G_{\mathbf{k}, \text{L}}^>(t) \right] \\ &\quad - 4 \sum_{\mathbf{q}, \mathbf{q}'} |w_{\mathbf{q}, \mathbf{q}'}|^2 \left[ \mathcal{G}_{\mathbf{q}, \text{L}}^<(-t) \mathcal{G}_{\mathbf{q}', \text{R}}^>(t) + \mathcal{G}_{\mathbf{q}', \text{R}}^<(-t) \mathcal{G}_{\mathbf{q}, \text{L}}^>(t) \right]. \end{aligned} \quad (28)$$

Collecting them and taking the Fourier transformation, we obtain

$$\begin{aligned} \mathcal{S} &= \mathcal{S}_{\text{qp}} + \mathcal{S}_{\text{pair}}, \quad (29) \\ \mathcal{S}_{\text{qp}} &= \int_{-\infty}^{\infty} \frac{d\omega}{2\pi} \sum_{\mathbf{k}, \mathbf{p}, \sigma} |t_{\mathbf{k}, \mathbf{p}, \sigma}|^2 \left[ G_{\mathbf{k}, \text{L}}^<(\omega) G_{\mathbf{p}, \text{R}}^>(\omega) + G_{\mathbf{k}, \text{L}}^>(\omega) G_{\mathbf{p}, \text{R}}^<(\omega) \right], \\ \mathcal{S}_{\text{pair}} &= -4 \int_{-\infty}^{\infty} \frac{d\omega}{2\pi} \sum_{\mathbf{q}, \mathbf{q}'} |w_{\mathbf{q}, \mathbf{q}'}|^2 \left[ \mathcal{G}_{\mathbf{q}, \text{L}}^<(\omega) \mathcal{G}_{\mathbf{q}', \text{R}}^>(\omega) + \mathcal{G}_{\mathbf{q}, \text{L}}^>(\omega) \mathcal{G}_{\mathbf{q}', \text{R}}^<(\omega) \right]. \end{aligned} \quad (30)$$

Using the relations associated with greater Green's functions

$$G_{\mathbf{p}, \text{j}}^>(\omega) = -i\mathcal{A}_{\mathbf{p}, \text{j}}(\omega)[1 - f_{\text{j}}(\omega)], \quad \mathcal{G}_{\mathbf{q}, \text{j}}^>(\omega) = -i\mathcal{B}_{\mathbf{q}, \text{j}}(\omega)[1 + b_{\text{j}}(\omega)], \quad (31)$$

and the lesser ones given by Eqs. (20) and (24), we obtain

$$\begin{aligned} \mathcal{S}_{\text{qp}} &= \int_{-\infty}^{\infty} \frac{d\omega}{2\pi} \sum_{\mathbf{k}, \mathbf{p}, \sigma} |t_{\mathbf{k}, \mathbf{p}, \sigma}|^2 \mathcal{A}_{\mathbf{k}, \text{L}}(\omega) \mathcal{A}_{\mathbf{p}, \text{R}}(\omega) [f_{\text{L}}(\omega) \{1 - f_{\text{R}}(\omega)\} + \{1 - f_{\text{L}}(\omega)\} f_{\text{R}}(\omega)] \\ \mathcal{S}_{\text{pair}} &= 4 \int_{-\infty}^{\infty} \frac{d\omega}{2\pi} \sum_{\mathbf{q}, \mathbf{q}'} |w_{\mathbf{q}, \mathbf{q}'}|^2 \mathcal{B}_{\mathbf{q}, \text{L}}(\omega) \mathcal{B}_{\mathbf{q}', \text{R}}(\omega) [b_{\text{L}}(\omega) \{1 + b_{\text{R}}(\omega)\} + b_{\text{R}}(\omega) \{1 + b_{\text{L}}(\omega)\}], \end{aligned} \quad (32)$$

which is equivalent to Eq. (6).

For a small bias limit at equal temperatures  $T_L = T_R \equiv T$  where  $\Delta\mu \rightarrow 0$  and  $f_R(\omega) \rightarrow f_L(\omega) \equiv f(\omega)$  with  $\mu_R \rightarrow \mu_L \equiv \mu$ , we obtain

$$f_L(\omega) - f_R(\omega) = -\frac{\partial f(\omega)}{\partial \omega} \Delta\mu + O((\Delta\mu)^2), \quad (33)$$

$$b_L(\omega) - b_R(\omega) = -2\frac{\partial b(\omega)}{\partial \omega} \Delta\mu + O((\Delta\mu)^2). \quad (34)$$

Using

$$f(\omega)\{1 - f(\omega)\} = -T\frac{\partial f(\omega)}{\partial \omega}, \quad b(\omega)\{1 + b(\omega)\} = -T\frac{\partial b(\omega)}{\partial \omega}, \quad (35)$$

we recover the Onsager's relation

$$S(\Delta\mu \rightarrow 0) = 2T\frac{I}{\Delta\mu}. \quad (36)$$

Moreover, the current and the noise can be rewritten as

$$I_{\text{qp}} = \int_{-\infty}^{\infty} \frac{d\omega}{2\pi} \sum_{\mathbf{p}, \mathbf{k}, \sigma} |t_{\mathbf{k}, \mathbf{p}}|^2 \mathcal{A}_{\mathbf{k}, \text{L}}(\omega) \mathcal{A}_{\mathbf{p}, \text{R}}(\omega) \left[ -\frac{1}{2} \frac{\sinh\left(\frac{\beta_{\text{L}}(\omega - \mu_{\text{L}}) - \beta_{\text{R}}(\omega - \mu_{\text{R}})}{2}\right)}{\cosh\left(\frac{\beta_{\text{L}}(\omega - \mu_{\text{L}})}{2}\right) \cosh\left(\frac{\beta_{\text{R}}(\omega - \mu_{\text{R}})}{2}\right)} \right], \quad (37)$$

$$I_{\text{pair}} = 2 \int_{-\infty}^{\infty} \frac{d\omega}{2\pi} \sum_{\mathbf{q}, \mathbf{q}'} |w_{\mathbf{q}, \mathbf{q}'}|^2 \mathcal{B}_{\mathbf{q}, \text{L}}(\omega) \mathcal{B}_{\mathbf{q}', \text{R}}(\omega) \left[ -\frac{1}{2} \frac{\sinh\left(\frac{\beta_{\text{b}, \text{L}}(\omega - \mu_{\text{b}, \text{L}}) - \beta_{\text{b}, \text{R}}(\omega - \mu_{\text{b}, \text{R}})}{2}\right)}{\sinh\left(\frac{\beta_{\text{L}}(\omega - \mu_{\text{b}, \text{L}})}{2}\right) \sinh\left(\frac{\beta_{\text{R}}(\omega - \mu_{\text{b}, \text{R}})}{2}\right)} \right], \quad (38)$$

$$\mathcal{S}_{\text{qp}} = \int_{-\infty}^{\infty} \frac{d\omega}{2\pi} \sum_{\mathbf{k}, \mathbf{p}, \sigma} |t_{\mathbf{k}, \mathbf{p}}|^2 \mathcal{A}_{\mathbf{k}, \text{L}}(\omega) \mathcal{A}_{\mathbf{p}, \text{R}}(\omega) \left[ -\frac{1}{2} \frac{\cosh\left(\frac{\beta_{\text{L}}(\omega - \mu_{\text{L}}) - \beta_{\text{R}}(\omega - \mu_{\text{R}})}{2}\right)}{\cosh\left(\frac{\beta_{\text{L}}(\omega - \mu_{\text{L}})}{2}\right) \cosh\left(\frac{\beta_{\text{R}}(\omega - \mu_{\text{R}})}{2}\right)} \right], \quad (39)$$

$$\mathcal{S}_{\text{pair}} = 4 \int_{-\infty}^{\infty} \frac{d\omega}{2\pi} \sum_{\mathbf{q}, \mathbf{q}'} |w_{\mathbf{q}, \mathbf{q}'}|^2 \mathcal{B}_{\mathbf{q}, \text{L}}(\omega) \mathcal{B}_{\mathbf{q}', \text{R}}(\omega) \left[ -\frac{1}{2} \frac{\cosh\left(\frac{\beta_{\text{L}}(\omega - \mu_{\text{b}, \text{L}}) - \beta_{\text{R}}(\omega - \mu_{\text{b}, \text{R}})}{2}\right)}{\sinh\left(\frac{\beta_{\text{L}}(\omega - \mu_{\text{b}, \text{L}})}{2}\right) \sinh\left(\frac{\beta_{\text{R}}(\omega - \mu_{\text{b}, \text{R}})}{2}\right)} \right]. \quad (40)$$

In particular, considering the large-biased limit where

$$\tanh\left(\frac{\beta_{\text{L}}(\omega - \mu_{\text{L}}) - \beta_{\text{R}}(\omega - \mu_{\text{R}})}{2}\right) \simeq \tanh\left(\frac{\beta_{\text{L}}(\omega - \mu_{\text{b}, \text{L}}) - \beta_{\text{R}}(\omega - \mu_{\text{b}, \text{R}})}{2}\right) \simeq 1, \quad (41)$$

is satisfied, we obtain

$$\mathcal{S}_{\text{qp}}(\Delta\mu \rightarrow \infty) \rightarrow I_{\text{qp}}, \quad \mathcal{S}_{\text{pair}}(\Delta\mu \rightarrow \infty) \rightarrow 2I_{\text{pair}}, \quad (42)$$

where we have denoted  $I \equiv I_{\text{qp}} + I_{\text{pair}}$ . The result of Eq. (42) motivates us to consider the Fano factor

$$F = \frac{S}{I} = \frac{\mathcal{S}_{\text{qp}} + \mathcal{S}_{\text{pair}}}{I_{\text{qp}} + I_{\text{pair}}}. \quad (43)$$

Then, one can see that the Fano factor  $F$  in a large-biased junction changes from 1 to 2 reflecting the ratio between  $I_{\text{qp}}$  and  $I_{\text{pair}}$ .

## RETARDED PROPAGATORS IN THE DILUTE RESERVOIR

For the single-particle Green's function in the reservoir R at dilute limit, we employ the non-interacting one given by

$$G_{\mathbf{p}, \text{R}}^{\text{ret.}}(\omega) = \frac{1}{\omega + i\eta - \epsilon_{\mathbf{p}}}, \quad (44)$$

where the self-energy correction is ignored [noting  $\epsilon_{\mathbf{p}} = p^2/(2m)$ ]. For the two-body sector, we can rewrite the lowest-order two-body propagator as

$$\Pi_{\mathbf{q},\mathbf{j}}^{\text{ret.}}(\omega) \equiv \Pi_{\mathbf{q},0}(\omega) + \Xi_{\mathbf{q},\mathbf{j}}(\omega), \quad (45)$$

where

$$\Pi_{\mathbf{q},0}(\omega) = \sum_{\mathbf{p}} \frac{1}{\omega + i\eta - \epsilon_{\mathbf{p}+\mathbf{q}/2} - \epsilon_{-\mathbf{p}+\mathbf{q}/2}} \quad (46)$$

and

$$\Xi_{\mathbf{q},\mathbf{j}}(\omega) = - \sum_{\mathbf{p}} \frac{f_{\mathbf{j}}(\epsilon_{\mathbf{p}+\mathbf{q}/2}) + f_{\mathbf{j}}(\epsilon_{-\mathbf{p}+\mathbf{q}/2})}{\omega + i\eta - \epsilon_{\mathbf{p}+\mathbf{q}/2} - \epsilon_{-\mathbf{p}+\mathbf{q}/2}} \quad (47)$$

are the in-vacuum two-body Green's function and the medium correction, respectively (for more details, see e.g., Refs. [34, 35]). Taking  $\alpha^2 = q^2/4 - m\omega - i\delta$ , we can analytically obtain

$$\Pi_{\mathbf{q},0}(\omega) = -\frac{m\Lambda}{2\pi^2} + \frac{m\alpha}{2\pi^2} \tan^{-1} \left( \frac{\Lambda}{\alpha} \right), \quad (48)$$

where  $\Lambda$  is an ultraviolet cutoff. Note that  $\Lambda$  is renormalized via

$$\frac{m}{4\pi a} = \frac{1}{g} + \frac{m\Lambda}{2\pi^2}, \quad (49)$$

which leads to

$$\begin{aligned} \frac{1}{\Gamma_{\mathbf{q},\mathbf{j}}^{\text{ret.}}(\omega)} &= \frac{m}{4\pi a} - \Pi_{\mathbf{q},\mathbf{j}}^{\text{ret.}}(\omega) - \frac{m\Lambda}{2\pi^2} \\ &\simeq \frac{m}{4\pi a} - \Xi_{\mathbf{q}}(\omega) - \frac{m\alpha}{4\pi} \end{aligned} \quad (50)$$

where the ultraviolet divergence is cancelled ( $\tan^{-1}(\frac{\Lambda}{\alpha}) \simeq \pi/2$  is used in the second line).

In the dilute limit, the fermionic medium correction  $\Xi_{\mathbf{q},\mathbf{R}}(\omega)$  is negligible. In this case, one can approximately obtain

$$\mathcal{G}_{\mathbf{q},\mathbf{R}}^{\text{ret.}}(\omega) \simeq \Pi_{\mathbf{q},0}(\omega) [1 - g\Pi_{\mathbf{q},0}(\omega)]^{-1}. \quad (51)$$

where  $\mathcal{G}_{\mathbf{q},\mathbf{R}}^{\text{ret.}}(\omega)$  does not involve any poles on the real frequency axis (i.e. bound states) at  $a^{-1} < 0$ . Note that the two-body continuum exists above  $\omega = q^2/(4m)$ . In the weak-coupling side ( $a < 0$ ), we obtain

$$\mathcal{B}_{\mathbf{q},\mathbf{R}}(\omega) = -2 \text{Im} \mathcal{G}_{\mathbf{q},\mathbf{R}}^{\text{ret.}}(\omega) = 0. \quad (\omega < q^2/4m). \quad (52)$$

Simultaneously, the frequency integration is restricted as  $\omega > 0$ . This fact indicates that particles in the reservoir L are transferred to the two-body continuum in the reservoir R via the two-body tunneling process in the weak-coupling side ( $a < 0$ ). On the other hand, in the strong-coupling limit ( $a \rightarrow +\infty$ ), we obtain [53, 55]

$$\mathcal{G}_{\mathbf{q},\mathbf{R}}^{\text{ret.}}(\omega) \simeq \left( \frac{m\Lambda}{2\pi^2} \right)^2 \frac{8\pi}{m^2 a} \frac{1}{\omega + i\eta - \frac{q^2}{4m} + E_{\text{b}}} \quad (\Lambda \rightarrow \infty), \quad (53)$$

which is proportional to the bosonic Green's function of a bound molecule with the binding energy  $E_{\text{b}} = 1/(ma^2)$ . Thus, in the strong-coupling regime ( $a > 0$ ), particles in the reservoir L can be transferred to the molecular bound states in the reservoir R via the two-body tunneling process.

## LARGE-BIAS LIMIT

In the main text, we considered a situation where fermions in the strongly-correlated reservoir L with a finite density  $N_{\text{L}}$  go through the tunneling junction to the dilute reservoir R with a vanishing density  $N_{\text{R}} \rightarrow 0$ , i.e.,  $\mu_{\text{R}} \rightarrow -\infty$  (see



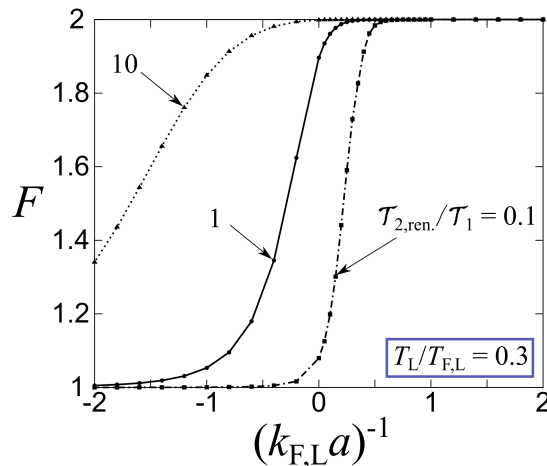


FIG. 5. Fano factor  $F$  throughout the BCS-BEC crossover at different tunneling-coupling ratio  $\mathcal{T}_{2,\text{ren.}}/\mathcal{T}_1$ . The temperature is taken as  $T_L/T_{F,L} = 0.3$ .

Fig. 1 in the main text). While we take the same temperatures  $T_L = T_R$  in the two reservoirs,  $T_R$  does not affect the result in the present case of  $\mu_R \rightarrow -\infty$  because the fugacity  $z_R = e^{\mu_R/T_R}$  characterizing the distribution vanishes regardless of the value of  $T_R$ . Indeed, we obtain vanishing  $N_R$  as [54]

$$N_R = 2z_R \left( \frac{2\pi}{mT_R} \right)^{\frac{3}{2}} + O(z_R^2) \rightarrow 0 \quad (z_R \rightarrow 0). \quad (54)$$

The number density  $N_L$  of the L-reservoir can be numerically obtained from

$$N_L = T_L \sum_{\mathbf{p}, \sigma, n} G_{\mathbf{p}, L}(i\omega_n). \quad (55)$$

In this regard, we normalize physical quantities by using the Fermi energy  $E_{F,L} = (3\pi^2 N_L)^{\frac{2}{3}}/(2m)$  and momentum  $k_{F,L} = (3\pi^2 N_L)^{\frac{1}{3}}$ .

## DIFFERENT TUNNELING-COUPLING RATIO

Figure 5 shows the calculated Fano factor  $F$  with different tunneling-coupling ratio  $\mathcal{T}_{2,\text{ren.}}/\mathcal{T}_1$  in the entire BCS-BEC crossover regime at  $T_L/T_{F,L} = 0.3$ . While in the main text we employed  $\mathcal{T}_{2,\text{ren.}}/\mathcal{T}_1 = 1$ , this ratio depends on the actual detailed setups in each experiment. If the two-body tunneling is relatively strong as  $\mathcal{T}_{2,\text{ren.}}/\mathcal{T}_1 = 10$ ,  $F$  is close to 2 even in the weak-coupling side [ $(k_{F,L}a)^{-1} \simeq -1$ ]. However,  $F$  decreases at weaker coupling even in this case. On the other hand, in the case with  $\mathcal{T}_{2,\text{ren.}}/\mathcal{T}_1 = 0.1$ ,  $F$  remains to be close to 1 even around unitarity. Nevertheless,  $F$  rapidly increases around  $(k_{F,L}a)^{-1} = 0.3$  and consequently reaches  $F = 2$  in the strong-coupling limit.

In this way, the detailed structure of the tunneling junction affects how  $F$  increases in the BCS-BEC crossover regime. However, our conclusion that  $F = 1$  and  $F = 2$  are achieved in the BCS and BEC limits, respectively, is unchanged even for different tunneling-coupling ratios. In other words, the pair tunneling process inevitably occurs in the strong-coupling regime even for an infinitesimally small pair-tunneling coupling  $\mathcal{T}_2$ . This is a natural consequence in the sense that the system is dominated by bound molecules and hence there are no single-particle states in such a regime.

\* hiroyuki.tajima@phys.s.u-tokyo.ac.jp

[1] L Amico, M Boshier, G Birkl, A Minguzzi, C Miniatura,

L-C Kwek, D Aghamalyan, V Ahufinger, D Anderson, N Andrei, *et al.*, “Roadmap on atomtronics: State of the art and perspective,” AVS Quantum Science **3**, 039201 (2021).

[2] Sebastian Krinner, Martin Lebrat, Dominik Hus-

- mann, Charles Grenier, Jean-Philippe Brantut, and Tilman Esslinger, “Mapping out spin and particle conductances in a quantum point contact,” *Proceedings of the National Academy of Sciences* **113**, 8144–8149 (2016).
- [3] Samuel Häusler, Shuta Nakajima, Martin Lebrat, Dominik Husmann, Sebastian Krinner, Tilman Esslinger, and Jean-Philippe Brantut, “Scanning gate microscope for cold atomic gases,” *Phys. Rev. Lett.* **119**, 030403 (2017).
- [4] WJ Kwon, G Del Pace, R Panza, M Inguscio, W Zwerger, M Zaccanti, F Scazza, and G Roati, “Strongly correlated superfluid order parameters from dc josephson supercurrents,” *Science* **369**, 84–88 (2020).
- [5] Niclas Luick, Lennart Sobirey, Markus Bohlen, Vijay Pal Singh, Ludwig Mathey, Thomas Lompe, and Henning Moritz, “An ideal josephson junction in an ultracold two-dimensional fermi gas,” *Science* **369**, 89–91 (2020).
- [6] G. Del Pace, W. J. Kwon, M. Zaccanti, G. Roati, and F. Scazza, “Tunneling transport of unitary fermions across the superfluid transition,” *Phys. Rev. Lett.* **126**, 055301 (2021).
- [7] Samuel Häusler, Philipp Fabritius, Jeffrey Mohan, Martin Lebrat, Laura Corman, and Tilman Esslinger, “Interaction-assisted reversal of thermopower with ultracold atoms,” *Phys. Rev. X* **11**, 021034 (2021).
- [8] L. Salasnich, N. Manini, and F. Toigo, “Macroscopic periodic tunneling of fermi atoms in the bcs-bec crossover,” *Phys. Rev. A* **77**, 043609 (2008).
- [9] M. Kanász-Nagy, L. Glazman, T. Esslinger, and E. A. Demler, “Anomalous conductances in an ultracold quantum wire,” *Phys. Rev. Lett.* **117**, 255302 (2016).
- [10] Juan Yao, Boyang Liu, Mingyuan Sun, and Hui Zhai, “Controlled transport between fermi superfluids through a quantum point contact,” *Phys. Rev. A* **98**, 041601 (2018).
- [11] François Damanet, Eduardo Mascarenhas, David Pekker, and Andrew J Daley, “Reservoir engineering of cooper-pair-assisted transport with cold atoms,” *New Journal of Physics* **21**, 115001 (2019).
- [12] M. Zaccanti and W. Zwerger, “Critical josephson current in bcs-bec-crossover superfluids,” *Phys. Rev. A* **100**, 063601 (2019).
- [13] Verdiana Piselli, Stefano Simonucci, and G Calvanese Strinati, “Josephson effect at finite temperature along the bcs-bec crossover,” *Physical Review B* **102**, 144517 (2020).
- [14] Shun Uchino, “Role of nambu-goldstone modes in the fermionic-superfluid point contact,” *Phys. Rev. Research* **2**, 023340 (2020).
- [15] F Setiawan and Johannes Hofmann, “Analytic approach to transport in josephson junctions beyond the andreev approximation: General theory and applications to the bec-bcs crossover,” *arXiv preprint arXiv:2108.10333* (2021).
- [16] Erich J Mueller, “Review of pseudogaps in strongly interacting fermi gases,” *Reports on Progress in Physics* **80**, 104401 (2017).
- [17] Shun Uchino and Masahito Ueda, “Anomalous transport in the superfluid fluctuation regime,” *Phys. Rev. Lett.* **118**, 105303 (2017).
- [18] Boyang Liu, Hui Zhai, and Shizhong Zhang, “Anomalous conductance of a strongly interacting fermi gas through a quantum point contact,” *Phys. Rev. A* **95**, 013623 (2017).
- [19] Yuta Sekino, Hiroyuki Tajima, and Shun Uchino, “Mesoscopic spin transport between strongly interacting fermi gases,” *Phys. Rev. Research* **2**, 023152 (2020).
- [20] Yuta Sekino, Hiroyuki Tajima, Masahito Ueda, Furutani and Yoji Ohashi, “Strong-coupling effects on quantum transport in an ultracold fermi gas,” *Journal of Low Temperature Physics* **201**, 49–57 (2020).
- [21] Hiroyuki Tajima, Daigo Oue, and Mamoru Matsuo, “Unified description of tunneling transport in ultracold atomic gases,” *arXiv preprint arXiv:2110.11701* (2021).
- [22] Ya. M. Blanter and M. Büttiker, “Shot noise in mesoscopic conductors,” *Phys. Rep.* **336**, 1 (2000).
- [23] T. Martin, “Noise in mesoscopic physics, in nanophysics: Coherence and transport, les houches session lxxxii,” (Elsevier, 2005) Chap. 5.
- [24] R. de Picciotto, M. Reznikov, M. Heiblum, V. Umansky, G. Bunin, and D. Mahalu, “Direct observation of a fractional charge,” *Nature* **389**, 162 (1997).
- [25] L. Saminadayar, D. C. Glattli, Y. Jin, and B. Etienne, “Observation of the  $e/3$  fractionally charged laughlin quasiparticle,” *Phys. Rev. Lett.* **79**, 2526–2529 (1997).
- [26] X. Jehl, M. Sanquer, R. Calemczuk, and D. Mailly, “Detection of doubled shot noise in short normal-metal/ superconductor junctions,” *Nature* **405**, 50 (2000).
- [27] A. A. Kozhevnikov, R. J. Schoelkopf, and D. E. Prober, “Observation of photon-assisted noise in a diffusive normal metal–superconductor junction,” *Phys. Rev. Lett.* **84**, 3398–3401 (2000).
- [28] O. Zarchin, M. Zaffalon, M. Heiblum, D. Mahalu, and V. Umansky, “Two-electron bunching in transport through a quantum dot induced by kondo correlations,” *Phys. Rev. B* **77**, 241303 (2008).
- [29] M. Ferrier, T. Arakawa, T. Hata, R. Fujiwara, R. Delagrè, R. Weil, R. Deblock, R. Sakano, A. Oguri, and K. Kobayashi, “Universality of non-equilibrium fluctuations in strongly correlated quantum liquids,” *Nature Physics* **12**, 230 (2016).
- [30] Akashdeep Kamra and Wolfgang Belzig, “Superpoissonian shot noise of squeezed-magnon mediated spin transport,” *Phys. Rev. Lett.* **116**, 146601 (2016).
- [31] Akashdeep Kamra and Wolfgang Belzig, “Magnon-mediated spin current noise in ferromagnet | nonmagnetic conductor hybrids,” *Phys. Rev. B* **94**, 014419 (2016).
- [32] M. Matsuo, Y. Ohnuma, T. Kato, and S. Maekawa, “Spin current noise of the spin seebeck effect and spin pumping,” *Phys. Rev. Lett.* **120**, 037201 (2018).
- [33] Joshua Aftergood and So Takei, “Noise in tunneling spin current across coupled quantum spin chains,” *Phys. Rev. B* **97**, 014427 (2018).
- [34] Giancarlo Calvanese Strinati, Pierbiagio Pieri, Gerd Röpke, Peter Schuck, and Michael Urban, “The bcs–bec crossover: From ultra-cold fermi gases to nuclear systems,” *Physics Reports* **738**, 1–76 (2018), the BCS–BEC crossover: From ultra-cold Fermi gases to nuclear systems.
- [35] Y. Ohashi, H. Tajima, and P. van Wyk, “Bcs-bec crossover in cold atomic and in nuclear systems,” *Progress in Particle and Nuclear Physics* **111**, 103739 (2020).
- [36] Shun Uchino, Masahito Ueda, and Jean-Philippe Brantut, “Universal noise in continuous transport measurements of interacting fermions,” *Phys. Rev. A* **98**, 063619 (2018).
- [37] Y Lubashevsky, E Lahoud, K Chashka, D Podolsky, and A Kanigel, “Shallow pockets and very strong coupling superconductivity in fese x te 1- x,” *Nature Physics* **8**,

- 309–312 (2012).
- [38] Shigeru Kasahara, Tatsuya Watashige, Tetsuo Hanaguri, Yuhki Kohsaka, Takuya Yamashita, Yusuke Shimoyama, Yuta Mizukami, Ryota Endo, Hiroaki Ikeda, Kazushi Aoyama, *et al.*, “Field-induced superconducting phase of fese in the bcs-bec cross-over,” *Proceedings of the National Academy of Sciences* **111**, 16309–16313 (2014).
- [39] Shahar Rinott, KB Chashka, Amit Ribak, Emile DL Rienks, Amina Taleb-Ibrahimi, Patrick Le Fevre, François Bertran, Mohit Randeria, and Amit Kanigel, “Tuning across the bcs-bec crossover in the multiband superconductor fe<sub>1-x</sub>se<sub>1+x</sub>: An angle-resolved photoemission study,” *Science advances* **3**, e1602372 (2017).
- [40] Tetsuo Hanaguri, Shigeru Kasahara, Jakob Böker, Ilya Eremin, Takasada Shibauchi, and Yuji Matsuda, “Quantum vortex core and missing pseudogap in the multiband bcs-bec crossover superconductor fese,” *Physical review letters* **122**, 077001 (2019).
- [41] Y. Nakagawa, Y. Saito, T. Nojima, K. Inumaru, S. Yamanaka, Y. Kasahara, and Y. Iwasa, “Gate-controlled low carrier density superconductors: Toward the two-dimensional bcs-bec crossover,” *Phys. Rev. B* **98**, 064512 (2018).
- [42] Yuji Nakagawa, Yuichi Kasahara, Takuya Nomoto, Ryotaro Arita, Tsutomu Nojima, and Yoshihiro Iwasa, “Gate-controlled bcs-bec crossover in a two-dimensional superconductor,” *Science* **372**, 190–195 (2021).
- [43] Jeong Min Park, Yuan Cao, Kenji Watanabe, Takashi Taniguchi, and Pablo Jarillo-Herrero, “Tunable strongly coupled superconductivity in magic-angle twisted trilayer graphene,” *Nature* **590**, 249–255 (2021).
- [44] Y. Suzuki, K. Wakamatsu, J. Ibuka, H. Oike, T. Fujii, K. Miyagawa, H. Taniguchi, and K. Kanoda, “Mott-driven bec-bcs crossover in a doped spin liquid candidate  $\kappa$ -(BEDT-TTF)<sub>4</sub>hg<sub>2.89</sub>brs,” *Phys. Rev. X* **12**, 011016 (2022).
- [45] Panpan Zhou, Liyang Chen, Yue Liu, Ilya Sochnikov, Anthony T Bollinger, Myung-Geun Han, Yimei Zhu, Xi He, Ivan Božović, and Douglas Natelson, “Electron pairing in the pseudogap state revealed by shot noise in copper oxide junctions,” *Nature* **572**, 493–496 (2019).
- [46] Ivan Božović and Jeremy Levy, “Pre-formed cooper pairs in copper oxides and laalo 3—srtio 3 heterostructures,” *Nature Physics* **16**, 712–717 (2020).
- [47] Koen M. Bastiaans, Damianos Chatzopoulos, Jian-Feng Ge, Doohee Cho, Willem O. Tromp, Jan M. van Ruitenbeek, Mark H. Fischer, Pieter J. de Visser, David J. Thoen, Eduard F. C. Driessen, Teunis M. Klapwijk, and Milan P. Allan, “Direct evidence for cooper pairing without a spectral gap in a disordered superconductor above  $t_c$ ,” *Science* **374**, 608–611 (2021).
- [48] Xinlong Han, Boyang Liu, and Jiangping Hu, “Enhancement of the thermal-transport figure of merit and breakdown of the wiedemann-franz law in unitary fermi gases,” *Phys. Rev. A* **100**, 043604 (2019).
- [49] Tomasz Sowiński, Mariusz Gajda, and Kazimierz Rzażewski, “Diffusion in a system of a few distinguishable fermions in a one-dimensional double-well potential,” *EPL (Europhysics Letters)* **113**, 56003 (2016).
- [50] J. Erdmann, S. I. Mistakidis, and P. Schmelcher, “Correlated tunneling dynamics of an ultracold fermi-fermi mixture confined in a double well,” *Phys. Rev. A* **98**, 053614 (2018).
- [51] See Supplemental Material at [http://link.aps.org/supplemental/10.1103/PhysRevLett.\\*\\*\\*.\\*\\*\\*\\*\\*](http://link.aps.org/supplemental/10.1103/PhysRevLett.***.*****) for a detailed information on detailed calculation of a current and noise, the single-particle Green’s function at dilute limit, and effect of the tunneling-coupling ratio.
- [52] Wilhelm Zwerger, *The BCS-BEC crossover and the unitary Fermi gas*, Vol. 836 (Springer Science & Business Media, 2011).
- [53] P. Pieri and G. C. Strinati, “Strong-coupling limit in the evolution from bcs superconductivity to bose-einstein condensation,” *Phys. Rev. B* **61**, 15370–15381 (2000).
- [54] Vudtiwat Ngampruetikorn, Meera M. Parish, and Jesper Levinsen, “High-temperature limit of the resonant fermi gas,” *Phys. Rev. A* **91**, 013606 (2015).
- [55] N. Andrenacci, P. Pieri, and G. C. Strinati, “Evolution from bcs superconductivity to bose-einstein condensation: Current correlation function in the broken-symmetry phase,” *Phys. Rev. B* **68**, 144507 (2003).